GSA Data Repository 2018026

Phillips et al., 2018, Determining the three-dimensional geometry of a dike swarm and its impact on later rift geometry using seismic reflection data: Geology, https://doi.org/10.1130/G39672.1.

Appendix A – Throw-depth analyses

T-z profiles can elucidate the kinematic history of normal faults (i.e. fault nucleation, growth, and/or reactivation) and thereby the tectonic evolution of sedimentary basins (see Mansfield and Cartwright, 1996; Cartwright et al., 1998 for a full description of the methods used). To assess how the Farsund Dike Swarm may have influenced the post-emplacement evolution of the study area, we calculated throw-depth (T-z) profiles along a number of key faults. We measure the hanging wall and footwall cut-offs of multiple stratigraphic horizons along the faults, plotting the calculated throw at the mid-point between the cut-offs. To accurately constrain the evolution of a fault, all fault slip-related strain must be explicitly recorded; i.e. we must incorporate both ductile (e.g. folding) and brittle (e.g. faulting) components of the strain field associated with fault slip (e.g. Meyer et al., 2002; Long and Imber, 2010; Whipp et al., 2014; Duffy et al., 2015; Jackson et al., 2017). Where fault-parallel folding occurs, hanging wall and footwall cut-offs were defined by projecting the regional dip of the horizon of interest, as measured some distance away from the fault, onto the fault plane.

Cartwright, J., Bouroullec, R., James, D., and Johnson, H., 1998, Polycyclic motion history of some Gulf Coast growth faults from high-resolution displacement analysis: Geology, v. 26, no. 9, p. 819-822.

Duffy, O. B., Bell, R. E., Jackson, C. A. L., Gawthorpe, R. L., and Whipp, P. S., 2015, Fault growth and interactions in a multiphase rift fault network: Horda Platform, Norwegian North Sea: Journal of Structural Geology, v. 80, p. 99-119.

Jackson, C. A.-L., Bell, R. E., Rotevatn, A., and Tvedt, A. B. M., 2017, Techniques to determine the kinematics of synsedimentary normal faults and implications for fault growth models: Geological Society, London, Special Publications, v. 439.

Long, J. J., and Imber, J., 2010, Geometrically coherent continuous deformation in the volume surrounding a seismically imaged normal fault-array: Journal of Structural Geology, v. 32, no. 2, p. 222-234.

Mansfield, C. S., and Cartwright, J. A., 1996, High resolution fault displacement mapping from three-dimensional seismic data: evidence for dip linkage during fault growth: Journal of Structural Geology, v. 18, no. 2–3, p. 249-263.

Meyer, V., Nicol, A., Childs, C., Walsh, J. J., and Watterson, J., 2002, Progressive localisation of strain during the evolution of a normal fault population: Journal of Structural Geology, v. 24, no. 8, p. 1215-1231.

Whipp, P. S., Jackson, C. A. L., Gawthorpe, R. L., Dreyer, T., and Quinn, D., 2014, Normal fault array evolution above a reactivated rift fabric; a subsurface example from the northern Horda Platform, Norwegian North Sea: Basin Research, v. 26, no. 4, p. 523-549.

Supplementary material

Figure DR1 – Map showing the locations of seismic reflection surveys used throughout this study

Figure DR2 – Map showing the locations of the interpreted dike swarm. Black lines represent sections of seismic data where dike-related reflections were identified

Figure DR3 – Uninterpreted seismic section for Figure 1c

Figure DR4 – Uninterpreted seismic section for Figure 2b

Figure DR5 – Uninterpreted seismic section for Figure 2c

Figure DR6 – Uninterpreted seismic section for Figure 2d

Table DR1 – Table showing the properties of the seismic reflection surveys used in this study

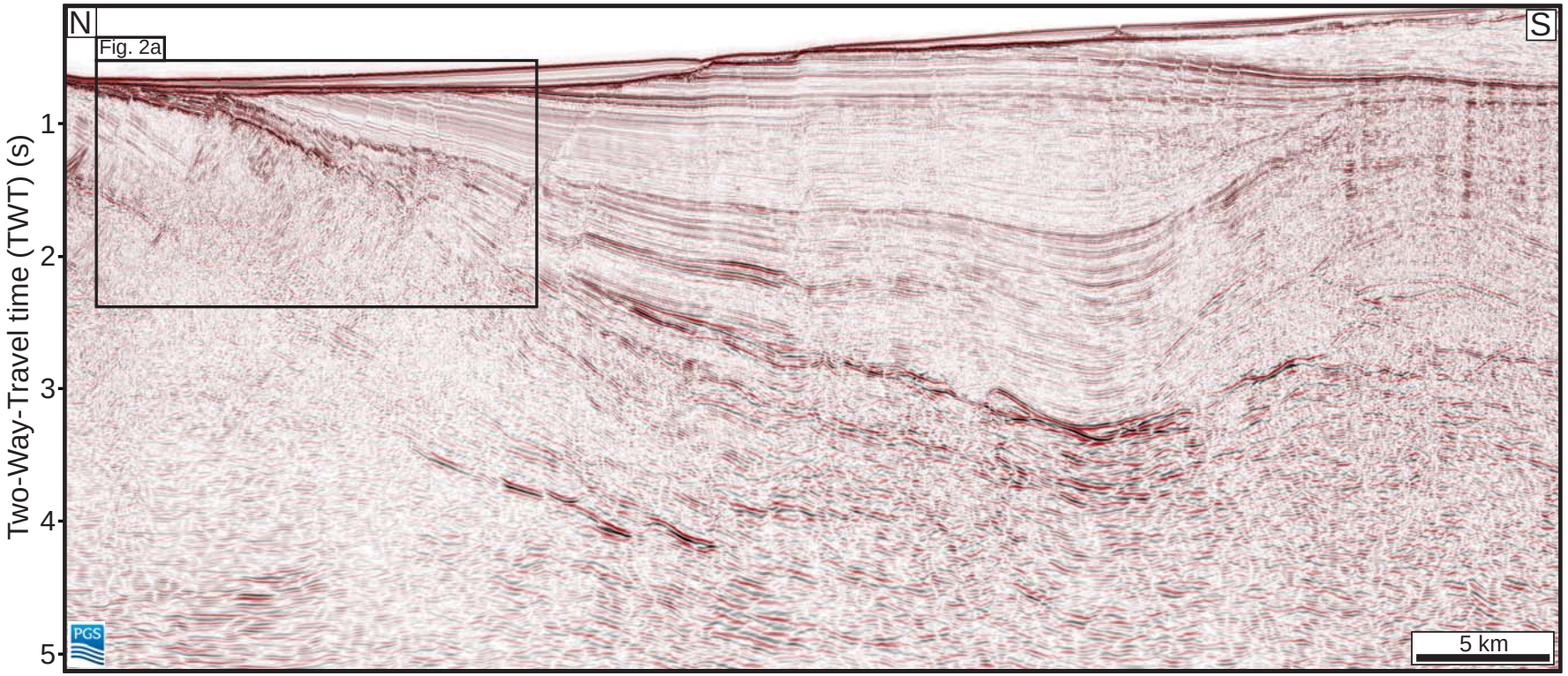

Fig. DR1

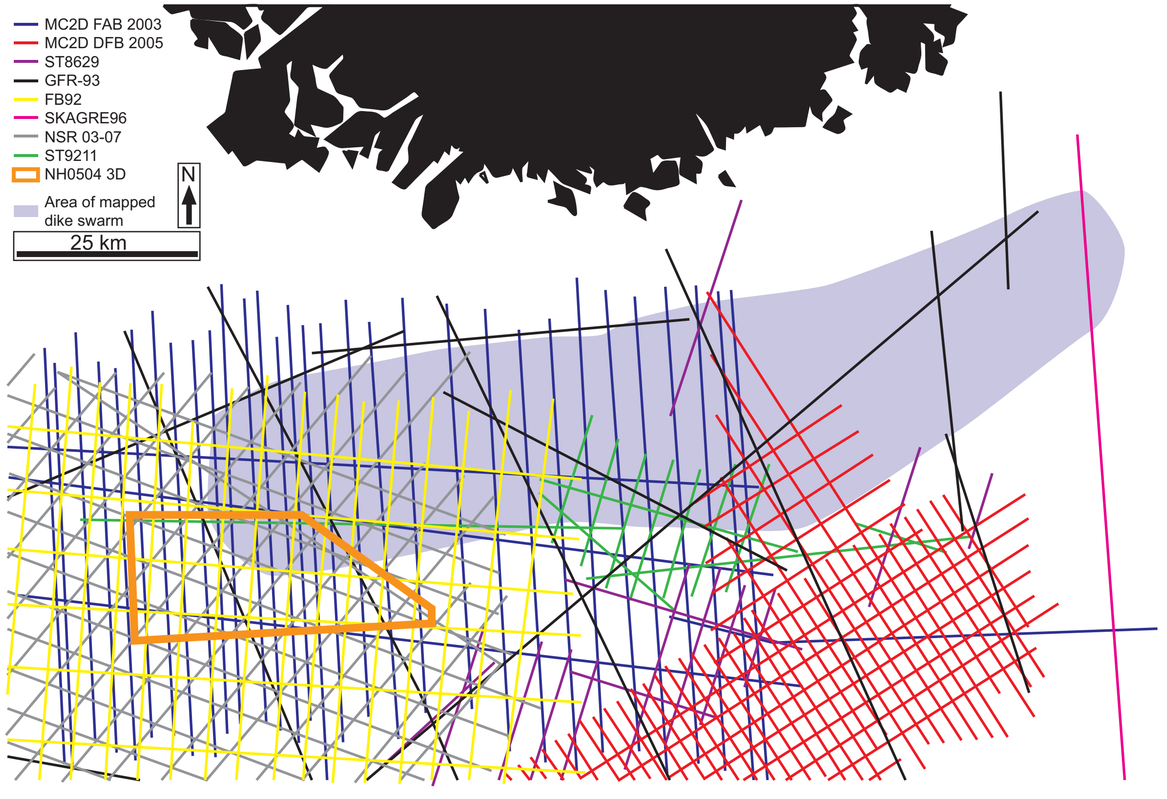
MC2D FAB 2003
MC2D DFB 2005
ST8629
GFR-93
FB92
SKAGRE96
NSR 03-07
ST9211
NH0504 3D
Area of mapped dike swarm
N
25 km

Figure DR2

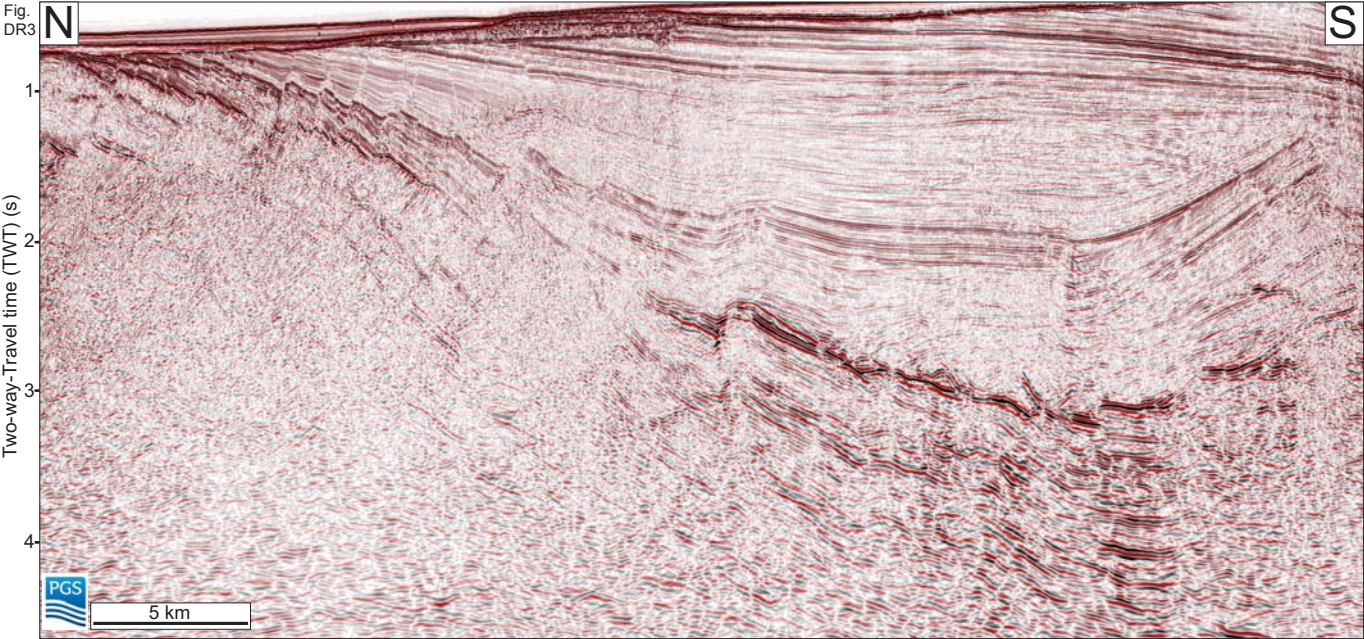
Fig. DR3
N
S
1
2
3
4
Two-way-Travel time (TWT) (s)
PGS
5 km

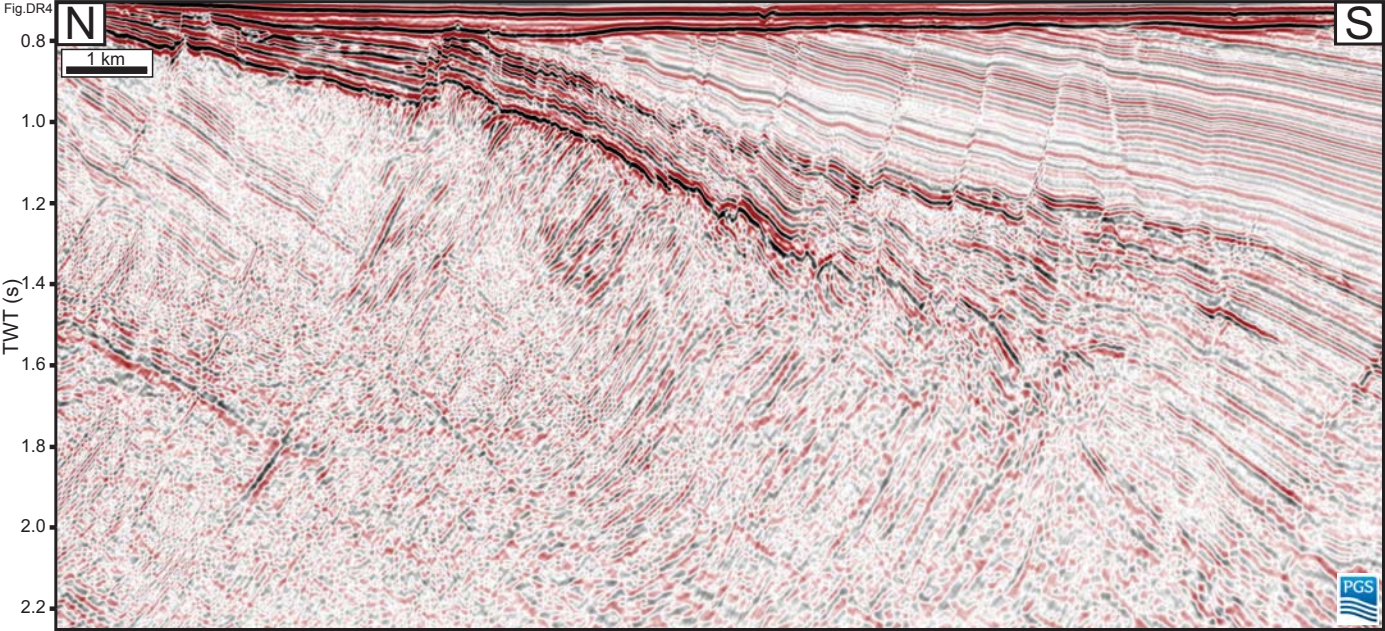
Fig.DR4
N
S
1 km
TWT (s)
0.8
1.0
1.2
1.4
1.6
1.8
2.0
2.2
PGS

Fig. DR5

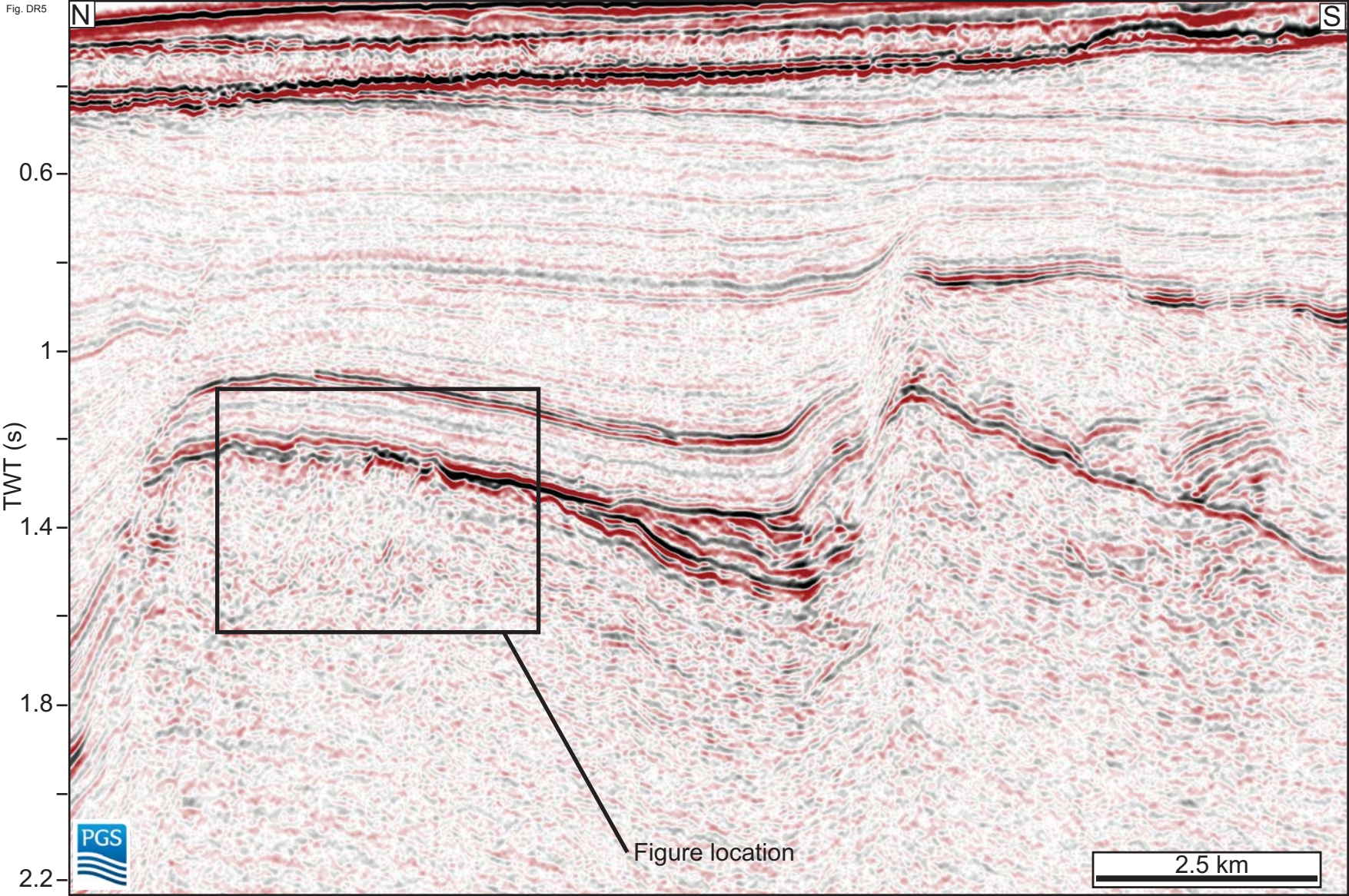

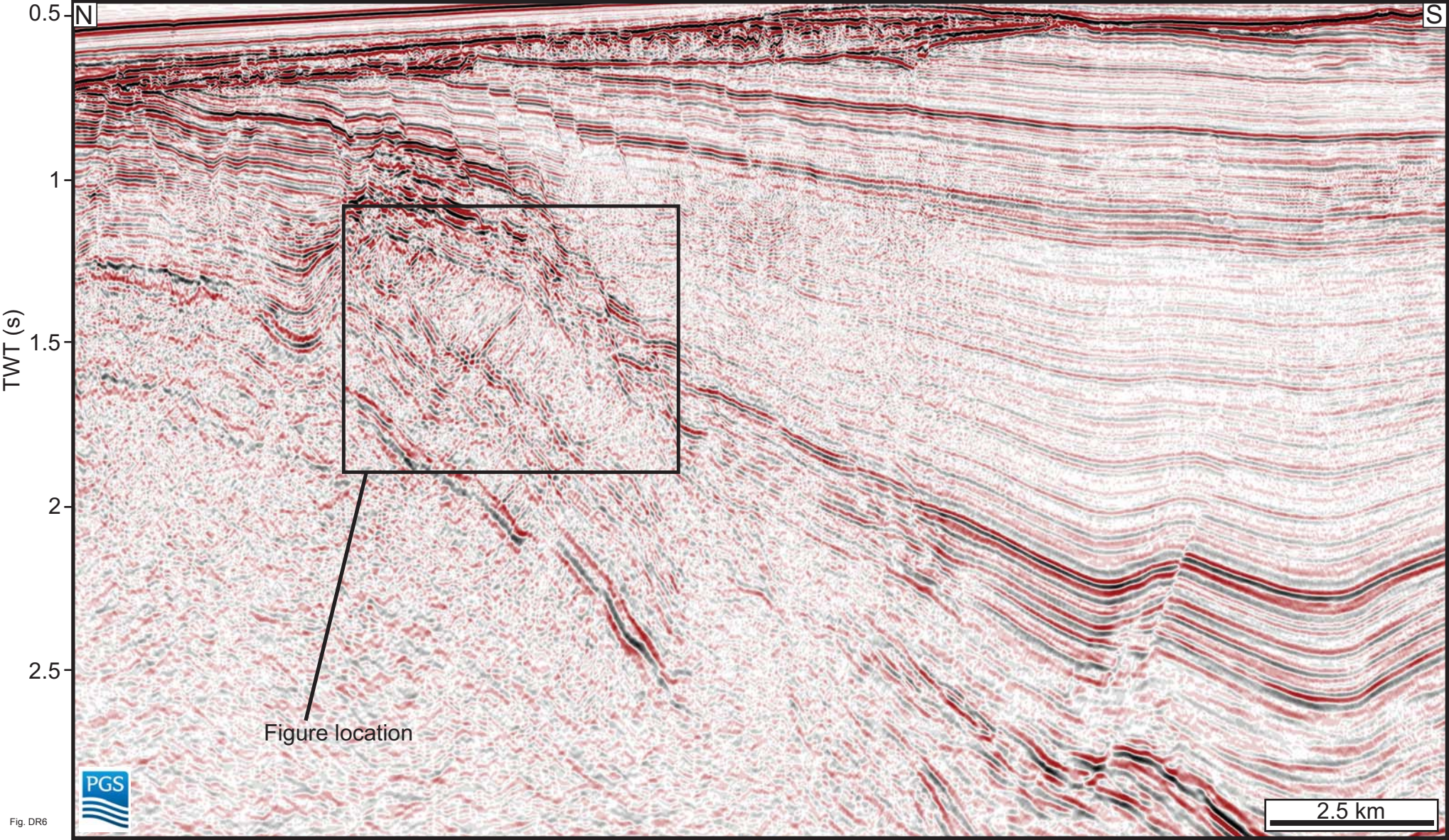

Fig. DR6

TABLE DR1

Dataset	Data type	Acquisition year	Record length (ms TWT)	Streamer length (m)	Fold	Shot interval (m)	Polarity (SEG convention)	Processing steps	
MC2D FAB 2003	2D	2003	7000	6000	120	25	Reverse	2D SRME	Hi-Res Rad/Kirchoff PSTM
MC2D DFB 2005	2D	2005	8000	6000	n/a	n/a	Reverse		
ST8629	2D	1986	6000	N/A			Reverse		
GFR-93	2D	1993	12000	4500			Reverse		
FB92	2D	1992	6000	N/A			Reverse		
SKAGRE96	2D	1996	7000	3000			Reverse		
NSR03-07	2D	2003-2007	9216	8087			Reverse		
ST9211	2D	1992	7000	3000			Reverse		
NH0504	3D	2005	4040	3000			Normal		

SRME	Surface related multiple elimination